*Fracture 1977, Volume 1, ICF4, Waterloo, Canada, June 19 - 24, 1977*

# THE PREDICTION OF CREEP FRACTURE IN ENGINEERING ALLOYS

D. McLean*, B. F. Dyson* and D. M. R. Taplin**


## ABSTRACT

*This paper examines the processes of microstructural degradation leading to intergranular creep fracture with the object of being able to provide a predictive metallurgical basis for problems of designing accurately for the complex conditions of creep encountered in modern engineering service. Creep and fracture under multiaxial stress states are first reviewed in detail to establish an appropriate base for an engineering theory of damage at high temperatures. Insight to be gained from metal science is then explored to provide the starting point for design life and residual life predictive schemes and the paper concludes with suggestions for new investigations. The overall orientation of the paper is to bring high temperature creep fracture into the main forum of applied fracture studies.*


## 1. INTRODUCTION

Without physical metallurgy, alloys are like "black boxes" whose interior is unknown and whose properties can be gauged only from external tests. Engineering design has perforce treated the problem of flow and fracture during service phenomenologically, mainly because the physical metallurgist has not oriented his studies of the inner workings of alloys in a predictive way. It has been argued that one must first understand the workings of simple alloys in simple situations before one can understand complex industrial alloys in realistic service conditions. This argument may prove to be false: at least, a situation of "overshoot" has developed. It now seems clear that if one wishes to provide useful predictive schemes - so that components and materials can be designed accurately for stringent and complicated service conditions at high temperatures - then the behaviour of these engineering materials must be studied under representative thermal and mechanical conditions. This means that the role of stress-strain needs to be considered as well as that of variable stress and temperature.

Coffin [1] has reviewed the broad field of variable stress at high temperatures; Greenwood [2] has considered the influence of variable temperature and stress on uniaxial creep fracture in pure metals whilst the paper by Dieter and Kuhn [3] examines hot fracture in bulk forming processes. Accordingly, the orientation of the present paper is towards the behaviour of industrially significant alloys subject to creep under uniaxial and multiaxial stress at constant temperature and will concentrate on those cases where fracture is a consequence of some internal material degradation or damage process - in particular, grain boundary cavitation. Failure caused by the influence of environment on material degradation will not

*National Physical Laboratory, Teddington, Middlesex, U.K.
**Department of Mechanical Engineering, University of Waterloo, Waterloo, Ontario, Canada.

be discussed since the essential assumption in this paper is that creep fracture is controlled by processes in the bulk of the alloy rather than at the surface. When failure is controlled by slow growth from a large pre-existing surface flaw, then clearly environmental effects are possible. Some studies have been made of such creep crack growth [4] but the focus of the present paper is upon situations where life is controlled by the formation of cracks less than approximately 5 mm in length.

The paper reviews the work done by engineers in predicting lifetime under homogeneous biaxial and non-homogeneous triaxial tensile stressing, describes the Kachanov damage accumulation theory and indicates the advantages of a metal science approach and how improvements to this theory can, and have been made from a knowledge of the physical cause of the internal damage process. The limitations of current understanding are discussed and some future research needs are outlined.

This Conference is concerned with the problem of *fracture* rather than *flow* - and *brittleness* rather than *ductility*. Fracture arises from a localization of flow so that it is, of course, necessary to study both these aspects of behaviour in order to gain a useful understanding. It is also important in studies of brittleness, cracks and fracture to maintain a clear overview of the specific problem in question. This is because the isolation of specific topics tends to be detrimental to progress - one loses sight of the applicability of new knowledge from one area of fracture to another. In fact, a prime example of this isolation is high temperature fracture. ICF has certainly neglected the problem of high temperature brittleness - perceiving it as somewhat outside the bailiwick of the Congress. Advances made at ordinary temperatures were *apparently* hardly relevant to high temperature service which, for many years, has been perceived as a special problem of no relevance to fracture mechanicians. ICF3 encouraged strong connections between problems of brittleness in the whole gamut of materials - rocks, polymers, glass, ceramics, concrete, metals, and composites. This policy continues in modified form at this conference but nonetheless the main thrust of the connections to be made at ICF4 is between the different classifications and types of fracture and between theory and engineering practice. Thereby, clear links can be established and parallels drawn between the various branches to produce generalized predictive criteria. It has been surely to the detriment of high temperature fracture that the links between all the various types of fracture have been neglected. One reason for this isolation of the problem arises from the belief, pursued fervently by many physical metallurgists, that creep fracture was largely controlled by vacancy-condensation. This approach does have its place, especially in irradiation conditions, but it now seems that it can only be applied to soft, model materials. It is only recently that the mainstream of fracture research has turned its attention to high temperatures and, albeit sparingly, attempted to extrapolate from low temperature work [5]. The Ashby Fracture Maps [6] and ICF4 overall should provide further impetus for the necessary broad approach to brittleness problems, the useful links existing between them and how fracture research can contribute to social aims.

One clear link exists between high temperature brittleness, which is largely intergranular, and the low temperature intergranular embrittlement examined by McMahon [7]. In his paper, McMahon chooses to classify fracture as *stress-controlled* and *strain-controlled*. Knott [5] provides a seemingly synonymous classification, *cracking processes* and *rupture processes*. Knott's classification may well be more generally useful





because no reason for the different types of behaviour is imputed before these have been identified. Accordingly, in high temperature processes, we need not depart from Knott's division. On the one hand, the brittle intergranular failure of a high strength superalloy at 973K gives the sure appearance of being a *cracking process* from the fracture surface (Figure 1), the tensile strain to fracture (less than 1%) and the sudden catastrophic release of stored elastic energy exhibited through the sound of the rapid, final fracture. In this instance, the cracking process seems to be stress-controlled and evidence has been put forward that the behaviour here is of the Griffith-Irwin type [8,9]. On the other hand, the sound of failure of a cavitating superplastic copper alloy at about 873 K is muted, the fracture is slow, the appearance is intergranular fibrous (Figure 2) and the tensile strain to fracture is about 500%. Everything here points to a *rupture process*, controlled by strain as well as material properties such as the strain-rate sensitivity and intercavity size and spacing. Goods and Nix [10] following the approach exemplified in Greenwood's paper [2] provide further evidence of a *rupture process* which is controlled by the normal stress across the boundaries. Also in the present conference, Jones and Pilkington [4] suggest that creep failure in a steel is a *cracking process* which is displacement or strain controlled. Accordingly in creep fracture we see that a classification based on cracking and rupture processes is appropriate but that in *each* case the process may be either stress or strain controlled.

A review written over ten years ago started from the different base of considering the overall problem of creep [11]. Even then, the conclusion was reached that the problem of fracture at high temperatures loomed larger than the problem of flow. It has taken over ten years to realize this and bring the problem of high temperature creep fracture to centre-stage in a major international fracture conference. Low temperature brittleness remains paramount in importance from the engineering viewpoint but it now seems that a fuller perspective has been achieved - both insofar as Fracture Mechanicians are perceiving creep fracture as an appropriate problem to work upon [12] and creep fracture researchers [9] are applying fracture mechanics, rather than just classical diffusional theory, to creep.

## 2. CREEP AND FRACTURE UNDER MULTIAXIAL STRESS

The principal objective underlying multiaxial creep testing of materials at high temperatures has been to develop economical but safe design methods suitable for engineering structures in which the stress system is invariably complex and therefore different from the uniaxial stress system normally used in the laboratory. It is therefore not surprising that the majority of work has been done by engineers of whom one man, A. E. Johnson, can be singled out for his pioneering research in this field. Johnson and his colleagues made a unique contribution towards understanding the mechanics of creep and fracture, particularly under spatially homogeneous and time independent biaxial loading. In section 2(a) this and other engineering work will be reviewed along with the much smaller contribution made by physical metallurgists. The latter have been interested principally in understanding the mechanisms of fracture but are becoming increasingly involved now in interfacing the mechanisms with the mechanics so that a better understanding can be achieved of the creep and fracture behaviour of engineering components and structures where temperature and stresses are spatially inhomogeneous and/or time dependent. Section 2(b) examines the recent progress which has been achieved in understanding the creep and fracture behaviour in one particular laboratory component in

which the stress is multiaxial, spatially inhomogeneous and time dependent: the uniaxially stressed circumferentially notched bar.

a) Biaxial stressing

Three testing methods have been used to assess both the creep and fracture behaviour of materials under approximately spatially uniform plane stress conditions viz: (i) combined tension and torsion of thin tubes, (ii) pressurised thin tubes with axial load and (iii) cruciform specimens. The work of Johnson and his colleagues [13,14] initially set out to discover the component or components of the stress tensor which would describe adequately primary and secondary creep deformation. They used the first of the above test methods and carried out systematic experiments at various constant temperatures, with a number of ratios of tensile to torsional stress, on two plain carbon steels, a low molybdenum alloy steel, an aluminium alloy (RR 59), Nimonic 75, a magnesium/aluminium alloy and commercially pure copper. Considerable effort was taken to ensure that the materials were isotropic, that there were at least 6 grains across the tube wall and that anisotropy was not introduced into the material by strain-hardening due to machining the thin walls of the tubes. For each material, at all temperatures it was found that the von Mises stress function $\sigma_M$ was the correct function concerned with the stress dependence of creep rate, where $\sigma_M$ is given by:

$$\sigma_M = D \left[(\sigma_1-\sigma_2)^2 + (\sigma_2-\sigma_3)^2 + (\sigma_3-\sigma_1)^2\right]^{1/2} \quad (1)$$

Here $\sigma_1$, $\sigma_2$ and $\sigma_3$ (= zero in these tests) are principal stresses and D is a numerical constant such that when $D = 1/3$ then $\sigma_M$ is termed the octahedral shear stress $\tau_{oct}$ and when $D = 1/\sqrt{2}$ then $\sigma_M$ is known as the effective stress $\bar{\sigma}$. $\bar{\sigma}$ is the most convenient definition since in a uniaxial test $\bar{\sigma}$ is equal to the applied stress. Their data showed that the effective primary and secondary creep strain rate $\dot{\bar{\varepsilon}}$ could be represented by:

$$\dot{\bar{\varepsilon}} = A(\bar{\sigma})^n f(t) \quad (2)$$

where $\dot{\bar{\varepsilon}} = \sqrt{2}/3\ [(\varepsilon_1-\varepsilon_2)^2 + (\varepsilon_2-\varepsilon_3)^2 + (\varepsilon_3-\varepsilon_1)^2]^{1/2}$ and $\varepsilon_1$ $\varepsilon_2$ $\varepsilon_3$ are principal strains. $f(t)$ was always a negative fractional power function of time in primary creep and of course equal to unity in secondary creep. In the middle and lower levels of stress n had a value between 1 and 2 for all materials and temperatures except for one of the carbon steels and the copper; in these two cases the n values were 2.2 and 4 respectively. All the materials obeyed the Lévy-von Mises rule that strain rate is in proportion to the magnitude of the deviatoric stress $\sigma'_{ij}$ given by:

$$\sigma'_{ij} = \sigma_{ij} + p\delta_{ij}$$

where p is the pressure and $\delta_{ij}$ is the Kronecker delta. Therefore, in its most general form, equation 2 becomes

$$\dot{\varepsilon}_{ij} = A'(\bar{\sigma})^{n-1}\sigma'_{ij}\ f(t) \quad (3)$$

Johnson preferred to use the second invariant of the deviatoric stress tensor $J_2$ to describe flow where $J_2$ is related to $\bar{\sigma}$ by a numerical constant and its index $p_1$ in Johnson's work is equal to $(n-1)$ in equation 3.





With one of the carbon steels a form of anisotropy occurred which could be represented by a simple variant of equation 3.

$$\dot{\varepsilon}_{ii} = A'(\bar{\sigma})^{n-1}\ [A'_{ij}(\sigma_{ii}-\sigma_{jj}) - A'_{ki}(\sigma_{kk}-\sigma_{ii})]\ f(t) \quad \text{etc.}$$

$A'_{ij}$ and $A'_{ki}$ are anisotropy coefficients which are constant for a given stress system and $\bar{\sigma}$ has an anisotropic value. Although exceptions to the Mises flow rule are reported occasionally (see for example Finnie and Abo El Ata [15]) equation 3 generally is accepted as describing deformation rate in primary and secondary creep.

The position with regard to creep fracture under steady multiaxial stressing is a more complicated one than that just outlined for creep deformation. Johnson's own work on the mechanics of creep fracture laid the foundations for current thinking on this subject in engineering circles. He and his colleagues showed, in a series of carefully designed experiments that the stress function describing fracture in the materials they investigated was either the Mises stress $\bar{\sigma}$ or the maximum principal stress $\sigma_1$. In arriving at this characterisation of materials they dismissed very elegantly an earlier theory of Siegfried [16] that intergranular failure was controlled by the hydrostatic stress. Furthermore they demonstrated that, for those materials characterised by $\bar{\sigma}$, a good representation of behaviour was given also by the criterion of fracture suggested by Kochendorfer [17]. For those materials characterised by $\sigma_1$ the Kochendorfer criterion obviously did not apply.

By analysing the shapes of their creep curves under multiaxial stress, Johnson and coworkers established that for $\bar{\sigma}$ materials the tertiary creep strain rate $\dot{\varepsilon}^t_{ij}$ could be described solely in terms of the Mises stress and, neglecting anisotropy, was given by:

$$\dot{\varepsilon}^t_{ij} = k(\bar{\sigma})^{n-1}\ \sigma'_{ij}\ f'(t) \quad (4)$$

Comparing equation 4 with equation 3 it is seen that, for $\bar{\sigma}$ materials, the only difference between the mechanics of creep strain in the primary, secondary and tertiary stages is the form of the function of time. The individual contributions to the measured strain rate may thus be expressed in terms of the octahedral plane creep strain rate as:

$$\dot{\bar{\varepsilon}} = A(\bar{\sigma})^n\ (B\ f(t) + C + D\ f'(t)) \quad (5)$$

where $Bf(t)$ represents primary creep, C secondary and $Df'(t)$ tertiary.

In contrast, for those materials whose fracture lifetime was characterised by $\sigma_1$ the tertiary creep strain rate was found to depend exponentially on a function of $\sigma_1$ only and could be represented by:

$$\dot{\varepsilon}^t_{ij} = k'f(\sigma_1)\ \sigma'_{ij}\ \exp^{K'f(\sigma_1)t}$$

where k' and K' are constants. For these materials therefore the expression equivalent to equation 5 is:

$$\dot{\bar{\varepsilon}} = A(\bar{\sigma})^n \left[B\ f(t) + C + \frac{k'f(\sigma_1)}{(\bar{\sigma})^{n-1}}\ \exp^{K'f(\sigma_1)t}\right] \quad (6)$$

Figure 3 illustrates schematically the shapes of creep curves predicted, for different values of

$$\frac{\sigma_1}{\bar{\sigma}}$$

by equation 6. A point to note is that no tertiary creep should occur in compression since

$$\frac{\sigma_1}{\bar{\sigma}}$$

is zero. Taira and Ohtani [18] obtained creep curves such as these by pressurising thin tubes and superimposing various axial loads, thereby changing

$$\frac{\sigma_1}{\bar{\sigma}}$$

and Johnson [13] and Finnie [15] have noted the absence of tertiary creep in compression.

In addition to considering the mechanics of creep and fracture under multiaxial stress Johnson also made qualitative observations, with an optical microscope, of 'cracking' on polished longitudinal sections of specimens tested to various fractions of rupture life. An exact definition of 'cracking' was not given but presumably what was meant was single and multiple grain facet cracks as defined in section 4. From these observations, he classified materials into two categories; (a) those whose rupture life was a function only of $\sigma_1$ and which exhibited spatially homogeneous grain boundary cracking which gradually accumulated during tertiary creep and (b) those whose rupture life was a function only of $\bar{\sigma}$ and which exhibited little or no cracking except in a small region adjacent to the fracture. In addition, the following points were also noted: (a) there was *not* a correlation between the *degree* of intergranular fracture and the stress component governing fracture lifetime. For example, fracture lifetime in RR 59 was governed by $\bar{\sigma}$ and yet all fractures were intercrystalline but in a 0.2% C steel, which was also controlled by $\bar{\sigma}$ all fractures were transgranular. Fracture lifetime in the Mo steel on the other hand was governed by $\sigma_1$ but all varieties of fracture were observed whereas in copper, which is also a $\sigma_1$ material, all the fractures were intercrystalline. (b) There was no correlation between tensile ductility and the stress component controlling fracture; a surprising result which was reinforced in later work by Henderson and Sneddon [19].

The loci of constant time to rupture (isochronous rupture surfaces) under plane stress condition for Johnson's two criteria have the form shown in Figure 4. The two criteria are almost indistinguishable in the tension-tension quadrant but their predictions diverge to a maximum in pure shear.

Hayhurst [20] has plotted the results of several biaxial rupture tests for 3 different engineering materials and concludes that a single isochronous surface describing their behaviour can be constructed by a combination of the hydrostatic stress and the Mises stress. The results themselves lie between the two isochronous surfaces in Figure 4.

Summarising the engineering work on the creep and fracture response of materials to steady plane stress loading, it has been established that primary and secondary creep deformation can be defined solely in terms of a shear stress ($\bar{\sigma}$) whereas tertiary creep deformation and fracture may require $\sigma_1$, $\bar{\sigma}$ or some combination of stress components. For





convenience, Leckie and Hayhurst [21] defined the terms $\phi/\phi$, to refer to those materials that obey equation 5, and $\phi/\Delta$ to refer to those obeying equation 6.

Until recently, physical metallurgists have paid scant attention to creep and fracture under multiaxial stress preferring, not surprisingly, to study the microstructural variables affecting fracture behaviour and using the uniaxial test as a means of quality assessment. Two studies [22,23] that consider stress state effects do exist however and, since they are both concerned with copper, they can be compared with the much larger amount of data found in the engineering literature, where this metal is thought of as a model $\phi/\Delta$ material. Table 1 summarises the important parameters. All the formulae for $t_f$ are expressed in exponential terms in deference to Johnson's original work even though some of the other data were published in terms of a power law. Surprisingly, in view of the dissimilar types of copper, grain size and the temperatures and modes of testing there is a similarity in the form of the expressions for $t_f$ in the works of Johnson et al, Kelly and Needham and Greenwood. All obey a $\sigma_1$ criterion of fracture and Leckie and Hayhurst would classify them as $\phi/\Delta$ materials. However, Needham and Greenwood [23] report, but do not quantify, a very marked dependence of minimum creep rate on $\sigma_1$ which is totally at variance with plasticity theory in general and the concept of $\phi/\Delta$ materials in particular. From Figures 1 and 2 in Needham and Greenwood's paper it is possible to work out an approximate expression for the minimum creep rate $\dot{\varepsilon}$ given by:

$$\dot{\varepsilon} = A\bar{\sigma}\,\sigma_1^{2.5} \qquad (7)$$

Another feature in Table 1 which is disturbing when related to the simple classification of materials outlined earlier in this section, is that in two of the investigations $t_f$ is explained better in terms of a function containing both $\sigma_1$ and $\bar{\sigma}$ although the discrepancy may be due simply to the very much shorter times to fracture in these two particular investigations.

(b) Triaxial tensile stressing

Since the aim of engineering work on creep and fracture is towards the better prediction of performance of structures, it is not surprising that there has been a considerable amount of component testing reported in the engineering literature. It is not the intention of this paper to review such work because, by its very nature, it is not generally suitable for quantitative treatment. However, advances in stress analysis over the last few years, due to the use of fast digital computers, have enabled studies to be made of the stress redistribution which takes place under conditions of triaxial states of stress, thereby allowing the possibility of quantitative fracture studies. Of the possible laboratory components from which to choose for a detailed analysis of the influence of triaxial stress on fracture the uniaxially loaded circumferentially notched bar has been selected since it has been recently subjected to stress analysis and is the most widely used laboratory technique for collecting data under a triaxial stress state.

Uniaxially loaded circumferentially notched bar test data are presently used as one of the qualitative guides in selecting the best available material for a specific structure but, as yet, they are not used to effect a more economical design of that structure. The reason why such data are used only in a qualitative way can be demonstrated by reference to Figure 5

which is a replot (to suit the present purpose) of some very comprehensive and systematically acquired results reported by Davis and Manjoine [26]. The ordinate is the ratio of the 1,000 h notch rupture strength to the 1,000 h plain bar rupture strength. Materials are said to exhibit 'notch weakening' if this ratio is less than unity and 'notch strengthening' if it exceeds unity. The abscissa is the ratio of notch radius 'r' to throat radius 'a'. Since 'a' is a constant, large values of a/r are a direct measure of notch acuity (sharpness). Four materials of widely different performance, as assessed by their uniaxial creep strengths and ductilities, were used and each material was tested over a wide range of notch acuities. All four materials exhibit notch strengthening when the notch is blunt but as its sharpness increases then three of the alloys eventually become notch weakened. There is a general correlation between behaviour and uniaxial ductility but this is not maintained in detail (for example compare alloys A and C).

Fracture behaviour such as that illustrated in Figure 5 is quite general but has not been quantified. In an attempt to provide a better understanding of notch behaviour Taira and Ohtani [27] have used a finite element procedure to calculate the transient and stationary state creep stress distributions in a circumferential 60° vee-notched bar. Only one notch geometry was discussed and the creep strain behaviour was assumed to follow, at all times, the Norton steady state creep law based on the von Mises flow criterion; primary and tertiary creep behaviour being neglected. Figure 6 shows, in schematic form, the spatial variation of the axial stress $\sigma_a$ and the effective stress $\bar{\sigma}$ as a function of the dimensionless parameter $x/a$ for times up to and including that for stationary state. Figure 6(c) shows quite clearly that the maximum value of the axial stress moves to a point some distance ahead of the notch root during creep and, in addition, $\bar{\sigma}$ becomes smaller than the nominal stress when stress redistribution is complete.

Hayhurst, Leckie and Henderson [28] have studied, by similar means, stress redistribution in circumferentially notched bars and their results confirm those of Taira and Ohtani but in addition, because they studied a variety of geometries their work is much more comprehensive. One particular notch geometry which they studied in detail gives the stationary state stress distribution illustrated in Figure 7. Here $\sigma_a$ rises monotonically to a maximum at the centre of the specimen while $\bar{\sigma}$ remains constant across the whole throat section and smaller in magnitude than the nominal stress. It is convenient to refer to this notch geometry as the 'Bridgman notch' since it was first analysed by Bridgman [29] for the case of time independent perfect plasticity. It is a general observation that stationary state stress redistributions in creep approximate closely to perfectly plastic solutions when the creep stress index 'n' is greater than about 5 and Hayhurst et al's work confirms this. Bridgman's [29] analytic expression for $\bar{\sigma}$ across the throat of a notch as a function of a/r is given by:

$$\bar{\sigma} = \sigma_{nom} \left[ \left( 1 + \frac{2r}{a} \right) \ln \left( 1 + \frac{a}{2r} \right) \right]^{-1}$$

If fracture lifetime is a function only of $\bar{\sigma}$ then the ratio of notched to un-notched rupture strength $\sigma_{nom}/\sigma_u$ is given by:

$$\frac{\sigma_{nom}}{\sigma_u} = \left( 1 + \frac{2r}{a} \right) \ln \left( 1 + \frac{a}{2r} \right)$$





$$\frac{\sigma_{nom}}{\sigma_u}$$

is plotted as a function of a/r in Figure 5. There is good agreement between the Bridgman notch strengthening prediction and the initial behaviour of three of the four alloys. There is an upper bound to notch strengthening due to the onset of gross section creep caused by the notch constraint and is given by

$$\frac{\sigma_{nom}}{\sigma_u} = (b/a)^2$$

where b is the radius of the plain section of the bar. This upper bound is shown as the line PQ in Figure 5 and is somewhat greater than the observed maximum strengthening. Another possible limit to strengthening is due to the ratio b/a being insufficient to sustain constraint beyond some critical value of a/r. From Figure 5, b/a = 1.33, and the maximum value of a/r for which full constraint can be maintained, can be calculated to be 1.5 (for method see Hayhurst [28]). This is shown as the line RS in Figure 5 and is below the observed maximum notch strengthening.

Although a qualitative explanation can be given for notch strengthening in terms of stationary state values of $\bar{\sigma}$ this cannot account for any tendency towards notch weakening as the notch acuity increases. One qualitative interpretation of this behaviour can be offered when account is taken of the calculations of Hayhurst et al [28] which show that the accumulated strain before a stationary state is reached is larger the sharper the notch. Thus beyond some critical notch acuity the accumulated strain may exceed locally that required for fracture before a stationary state is reached. The more ductile the material the sharper the notch must be before such transient effects intervene, in agreement with the general trend of the results in Figure 5. As already noted, uniaxial ductility values do not give detailed agreement and any quantitative theory that eventually emerges will almost certainly require a knowledge of the effect of triaxial tensile stress on ductility in order to establish a failure criterion. Quantitative studies of ductility under triaxial tensile stress may be achieved by using a Bridgman notch where, as Figure 7 shows, a reasonably uniform triaxial stress state can be maintained over a large part of the notch throat. In carrying out such experiments in creep care must be taken to ensure that the value of the creep exponent is sufficiently high to effect this stress distribution.

## 5. ENGINEERING THEORY OF DAMAGE

The accelerating stage of constant temperature creep called tertiary which eventually ends in fracture has led to the concept of damage accumulation. A method of quantifying this progressive development of damage was introduced by Kachanov [30] and a readable account in English has been published recently by Penny [31]. The original procedure was designed for uniaxial stressing by defining a parameter w which can be regarded as reducing the effective cross-sectional area by the fractional amount w, although some workers, for example Leckie and Hayhurst [21] prefer a less restricted definition. In a uniaxial situation the actual stress at a given moment is $\sigma_0/(1-w)$ where $\sigma_0$ is the initial value. For moderate changes in stress, Norton's law is an acceptable approximation to the secondary creep rate. Thus we can describe the secondary and

tertiary stage of creep by the following equation:

$$\dot{\varepsilon} = A\left[\frac{\sigma_o}{1-w}\right]^n \qquad (8)$$

A and n are the constants and equation (8) reduces to the standard Norton equation for secondary creep rate when w = o. As the parallel equation for the damage rate $\dot{w}$, Kachanov assumed:

$$\dot{w} = B\left[\frac{\sigma_o}{1-w}\right]^p \qquad (9)$$

where B and p are constants.

In the original formulation of this theory the power indices of $\sigma_o$ and of (1-w) in equations 8 and 9 were not regarded as necessarily equal, perhaps out of a natural inclination to introduce extra adjustable parameters that would allow a good fit with experimental data. Here for simplicity they are taken as equal. This seems a logical consequence of our definition of (1-w) as the stress-bearing fraction of the cross-section but the assumption is clearly questionable.

As the first test of this theory one might ask how well it can represent $\varepsilon/t$ relations in creep. Following Rabotnov [32] and suitably manipulating equations 8 and 9, it is found that

$$\frac{\varepsilon}{\varepsilon_f} = 1 - \left(1 - \frac{t}{t_f}\right)^{\frac{1+p-n}{1+p}} \qquad (10)$$

where $\varepsilon_f$ and $t_f$ are respectively the elongation and time at fracture. Equation 10 represents accelerating creep, as is evident from the basis of the theory that it should.

To compare equation 10 with experimental data, therefore, the primary creep must be subtracted first, unless it is negligible, as often is the case with engineering alloys. Penny [31] has shown that equation 10 can well represent the $\varepsilon/t$ data of Al alloys; his example is reproduced as Figure 8, which shows very good agreement, at least up to 0.95 $t_f$, in this case where primary creep is negligible and where also n = p = 5. However, equation 10 does not always fit the data so well. The solid line in Figure 9 is the experimental $\varepsilon/t$ curve for tensile creep of the alloy Nimonic 80A - it can be seen here that primary creep again makes a negligibly small contribution to the total creep strain and the dashed lines are obtained from equation 10 with alternative exponents. Evidently good agreement with experiment is not possible. However, if the last 10% of life is neglected, i.e. if w = 1 at t = 1600 h and $\varepsilon_f$ = 6.3%, the fit is much improved over the first 90% of life as the dotted line shows. In this way equations 8 and 9 will probably often represent most of the $\varepsilon/t$ relation as long as primary creep is insignificant.

A second test of the theory concerns its ability to predict the effect of variable conditions. Proceeding by analogy with creep strain, the damage could be, in principle, either damage-caused-by-strain or damage-caused-by-time if the analogy is drawn with "strain-hardening" and "time-hardening" theories of creep. From equations 8 and 9 and taking n = p, $\dot{w}$ can be expressed as:

$$\dot{w} = B\,\sigma^n\,(1+n)\,\left(1 - \frac{\varepsilon B}{A}\right)^n \qquad (11)$$





or

$$\dot{w} = B\,\sigma^n \Big/ \left[1 - B\,\sigma^n\,(1+n)t\right]^{\frac{n}{1+n}} \qquad (12)$$

Equation 11 is the "strain-damage" expression and equation 12 is the "time-damage" expression. Just as strain-hardening and time-hardening theories predict a different response of $\dot{\varepsilon}$ to change of stress, equations 11 and 12 predict a different response of $\dot{w}$. Thus, suppose the initial applied load remains fixed until the strain $\varepsilon'$ is reached at time t', and the applied load is then increased. Just before the increase, equations 11 and 12 give the same value of w. However, $\dot{w}$ is less sensitive to stress in equation 11 than in equation 12, and consequently if the damage is strain dependent the increase in w is less than if it were time dependent. The two concepts thus yield different summation rules.

Imagine a test in which an applied stress $\sigma_1$ is held for time $t_1$, producing strain $\varepsilon_1$ and damage $w_1$, and then the applied stress is changed to $\sigma_2$ until fracture occurs at time $t_2$ and strain $\varepsilon_2$. The time-damage concept yields $t_1/t_{1f} + t_2/t_{2f} = 1$, which is Robinson's law, and the strain-damage concept yields $\varepsilon_1/\varepsilon_{1f} + \varepsilon_2/\varepsilon_{2f} = 1$, the suffix f denoting fracture in each case. Engineering science cannot measure w directly, and consequently to decide between the strain- and time-concepts, or to decide whether either is correct, would have to draw an inference from a measured quantity such as the strain/time relation. As we shall see, metal science is able to help by identifying and also measuring w directly.

A third test is the ability to predict the effect of multi-axial stress, with which this article is mainly concerned. Since the cavities and cracks of which w is some measure often lie preponderantly on grain boundaries nearly normal to the maximum principal stress $\sigma_1$, it is reasonable to write, as Rabotnov [32] does, the three principal stresses as $\sigma_1/(1-w)$, $\sigma_2$, $\sigma_3$, the two smaller ones being unaltered by the damage. Equation 8 now becomes:

$$\dot{\varepsilon}_1 = A'(\bar{\sigma})^{n-1}\,\sigma_1' \quad \text{etc} \qquad (13)$$

where $\bar{\sigma}$ is again the effective stress, which in the present case is given by:

$$\bar{\sigma} = \frac{1}{\sqrt{2}}\left[\left(\frac{\sigma_1}{1-w} - \sigma_2\right)^2 + (\sigma_2-\sigma_3)^2 + \left(\sigma_3 - \frac{\sigma_1}{1-w}\right)^2\right]^{1/2} \qquad (14)$$

A' is the new appropriate constant and $\sigma_1'$ is the maximum deviatoric stress. Equation 13 reduces to equation 8 for uniaxial tension. As for equation 9, however, *a priori* it could remain either unaltered or take the form:

$$\dot{w} = B'(\bar{\sigma})^r \qquad (15)$$

the first choice (which Kachanov himself uses) implying that damage is caused to grow by the maximum principal stress and the second that damage is caused to grow by strain, when B' is the new appropriate constant. Either of these choices seems much more suitable here than pure time-dependent damage because the variable *time* is not in itself the determining parameter.

A useful prediction is that of the fracture lifetime $t_f$. With the first choice it is obtained by integrating equation 9 to find:

$$t_f = \frac{1}{B(\sigma_1)^r}\int_0^1 (1-w)^r\,dw = \frac{1}{B\sigma_1^p(1+p)} \qquad (16)$$

Line A in figure 10 is the isochronous rupture surface in plane stress obtained from equation 16; it lies at constant $\sigma_1$ with this choice since this first choice makes $t_f$ depend only on maximum principal stress. With the second choice $t_f$ is similarly obtained by integrating equation 15, which was done numerically after writing $\bar{\sigma} = \sigma_1 [1/(1-w)^2 - f/(1-w) + f^2]^{1/2}$ where the stresses are $\sigma_1/(1-w)$, $\sigma_2 = f\,\sigma_1$, $\sigma_3 = 0$ (i.e. plane stress). Line C in Figure 10 is the isochronous surface so obtained with $n = p = 4$. As was mentioned in section 2 many data points lie between lines A and C, which implies that the correct expression for $\dot{w}$ lies between equation 9 and equation 15. As long as the metal is regarded as a black box, however, the only way of obtaining a more exact expression is by trial and error.

Leckie and Hayhurst [21] seem to be the only researchers who have used the Kachanov damage concept to derive expressions giving the time to first cracking of *structures* operating at constant temperature. Their derivations of these lower bound expressions of failure times incorporate the classification of materials into $\phi/\phi$ and $\phi/\Delta$ types defined in section 2(a) as well as taking account of both stress redistribution and multiaxial stress states. The failure times are expressed in terms of an equivalent representative rupture stress which allows failure times to be obtained from uniaxial stress rupture data. Experimental evidence in support of their theory was obtained by testing copper and an aluminium alloy in four component forms.

## 4. INSIGHT FROM METAL SCIENCE

By examining the processes which go on inside the alloy black box, metal science can learn to identify the damage and how to handle it for predictive purposes by determining which are the correct stress components for use in the constitutive equations describing damage accumulation [33]. As a result of this extra insight, extrapolation should be more reliable and thereby reduce the amount of expensive large scale testing. This section indicates some ways in which progress is being made.

### (a) Damage mechanisms

Metal science can distinguish between those internal damage processes that 'soften' the material and thus cause the creep rate to increase and thereby indirectly induce failure and those that are directly responsible for the actual fracture of the material. The former include dislocation recovery, recrystallisation, matrix solute depletion (by precipitation in ineffective form) and coarsening of second phase particles. Damage due to particle coarsening has been shown to be an important cause of decreased flow resistance [34] and is the only one to receive quantitative evaluation [35]. Figure 11 illustrates this by showing how the creep rate of one type of steel used for power station superheaters increases as the precipitate particles coarsen and thus become more widely spaced [35]. Such studies have recently become more feasible since measurements of particle spacing can now be made accurately with the high voltage electron microscope.

The internal damage ultimately responsible for intergranular creep fracture starts as individual grain boundary cavities. These cavities multiply and grow to form cracks on individual grain surfaces [single grain facet (sgf) cracks] which, in turn, link together to form a final fatal crack. The nomenclature which has been used in this extensively studied area (for a recent review see Perry [36]) is far from standardised and the use of





the word 'crack' must not be taken too literally since, to cover the observations which have been reported in the literature, the 'crack' shape may be that of an oblate or prolate spheroid. Nevertheless, the sequence described above appears to be quite general if the material does in fact fail intergranularly. Although in the past the major engineering objective of experimental physical metallurgical work in this area has been to improve the creep fracture resistance of complex alloys by altering their microstructure, this research has been valuable nevertheless in establishing the necessary framework for service life prediction methods. For example, a disproportionate increase in fracture ductility is achieved by effecting small changes in the trace element composition of Cr-Mo-V steels [37]. Similarly, fracture ductility is markedly improved by reducing the grain size [8]. In each of these examples, the common feature responsible for improved performance is related to the degree or distribution of intergranular damage. In the first example, purity influences directly the cavity nucleation rate and hence the rate of formation of sgf cracks; in the second, small grain size influences the ability of sgf cracks to link to form a critical multiple grain facet (mgf) crack. From a predictive viewpoint the initial problem is to decide which of the two stages, formation of sgf cracks by individual cavity nucleation and growth or formation of a critical mgf crack is rate controlling. An assessment of the current situation with regard to predictive theories will be made in a later section.

### (b) Stress components

As far as plastic creep strain is concerned, the best approximation to the correct stress which is available from metal science is the Taylor-Bishop-Hill [38] stress $\tau_T$. However, with randomly oriented polycrystals in the fcc system this does not differ much from the octahedral shear stress $\tau_{oct}$ of engineering science in that, for all stress systems, the ratio $\tau_T/\tau_{oct}$ lies within ± 5%. Moreover, at elevated temperature additional processes of deformation are possible - diffusion creep, grain boundary sliding, slip on additional planes - which should reduce even further the relative variation between $\tau_T$ and $\tau_{oct}$. For practical purposes, therefore, as far as creep deformation is concerned $\tau_{oct}$ is a perfectly acceptable replacement for $\tau_T$, at least with most metals, and is much easier to calculate. In regard to the significant stress component for plastic creep strain metal science and engineering science thus come to the same conclusion.

For creep fracture on the other hand the conclusions from metal science go further than those from engineering science. One must consider the stages of creep fracture referred to in the previous section:

(i) Cavities are nucleated as a consequence of plastic strain and all micromechanisms require a concentrated normal traction in a local region by means of shear stress relaxation against a suitable obstacle. The plastic strain may be due to transgranular slip or grain boundary sliding: Figure 12 shows examples of nucleation processes which have varying degrees of experimental support [8,9,39,40]. One stress component determining the rate of nucleation is therefore $\bar{\sigma}$ (or $\tau_{oct}$). Such mechanisms as those envisaged in Figure 12 will inevitably produce a spectrum of initial cavity sizes but, for growth to occur by vacancy condensation from adjacent sinks, thermodynamics imposes a constraint on their continued stability since the *minimum* size of cavity able to grow is given by $r = 2\gamma/\sigma_n$ where $\gamma$ is surface energy and $\sigma_n$ is the local traction acting on a vacancy sink. Neglecting any interior stress redistribution, the

minimum r occurs when $\sigma_n$ is the largest applied direct stress i.e. the maximum principal stress $\sigma_1$ in a triaxial stress state, for example. When the vacancy sinks lie on grain boundaries then even though there may be a random distribution of cavities produced by shear, on boundaries perpendicular to the direction of $\sigma_1$ cavities will be more stable. This is often observed in practice. The significant applied stress components for nucleation when continued growth is by vacancy condensation are therefore $\bar{\sigma}$ and $\sigma_1$. However when continued growth is by a viscous (i.e. power law creep) mechanism (see (ii) below), the stability criterion is $2\gamma/\sigma_m$, where $\sigma_m$ is the hydrostatic stress, and the significant stress components then become $\bar{\sigma}$ and $\sigma_m$. In either situation, cavitation will not occur under purely hydrostatic stress since $\bar{\sigma}$ is then zero and no shear can occur. When nucleation occurs by cracking of hard particles this stability criterion may not apply.

(ii) The kinetics of continued growth of individual cavities on single grain boundary facets has aroused considerable controversy over the years. The issue has been polarised into two camps, one favouring a volume growth rate linearly proportional to $\sigma_1$, (e.g. Speight and Harris [41]), whilst the other favours a growth rate proportional to strain rate and therefore non-linearly related to $\bar{\sigma}$ (e.g. Davies and Wilshire [42]). Little direct evidence exists to support unambiguously either view. Both types of growth rate law can be obtained using the Balluffi-Seigle stress directed vacancy concept; the $\sigma_1$ law results when the mean normal traction across a boundary transverse to $\sigma_1$ is equal in magnitude to $\sigma_1$ [41] while two mechanisms have been proposed to account for a deformation rate dependence. The first [43] of these assumes that the vacancy sinks are dislocations arriving at a grain boundary from the grain interior during creep and that their rate of arrival controls the kinetics. The second [44] uses the fact that cavitated boundaries are usually distributed inhomogeneously and that the consequent inhomogeneous stress can result again in their growth rate being controlled by the deformation rate of surrounding non cavitated grains. It is interesting to conclude therefore that although the *mechanics* of growth may be either $\sigma_1$ or $\bar{\sigma}$ controlled, the *mechanism* in each case can be related to stress directed diffusion of vacancies. Both types of growth kinetics are thus compatible with the ideas on cavity nucleation discussed in the previous section.

There is a further deformation controlled cavity growth mechanism that is not based on the Balluffi-Seigle concept and which has been applied in detail recently to creep cavities by Hancock [45] and applied by Fleck et al [9] to cavitation in fine grained materials. This is the viscous hole growth mechanism usually associated with room temperature ductile fracture: in the creep situation plastic growth is controlled by power-law creep. The local stress components which are significant for this mechanism are $\bar{\sigma}$ and the ratio

$$\frac{\sigma_m}{\bar{\sigma}} \quad .$$

Nucleation of cavities by a random shear mechanism as discussed above would produce an observable random distribution of cavities if the local stress tensor were spatially uniform since the stability criterion is $2\gamma/\sigma_m$. This contrasts with the non-random distribution forecast by application of the Balluffi-Seigle stability criterion. To illustrate the probable range of applicability of viscous cavity growth under uniaxial creep conditions Dyson and Taplin [33] derived Figure 13 by plotting the locus of points of equal growth rate given by:





$$\dot{R} = \dot{\epsilon} R \tag{17}$$

and

$$\dot{R} = \frac{D_b \sigma_1 \Omega\delta}{2kTR^2 \ln\left(\frac{a}{2R} - \frac{1}{2}\right)} \tag{18}$$

where equation 17 is given by Hancock [45] for the growth rate $\dot{R}$ at radius R under uniaxial strain rate $\dot{\epsilon}$. Equation 18 is Speight and Harris's [41] formulation of diffusive growth for cavities of spacing 'a'. Figure 13 was derived by inserting typical values for the various parameters for fcc materials and assuming a = 10 μm. Viscous hole growth is unimportant at engineering strain rates of $10^{-10}$ $s^{-1}$ but under fast laboratory tests, particularly at low homologous temperatures it becomes the dominant mechanism at relatively low values of 2R/a. This process of growth is also highly stress state dependent and may become dominant at crack tips due to locally high strain-rates and stress states. It should be noted that when 'a' is changed the curves are translated so that larger 'a' values favour viscous growth. In view of the general nature of the parameters used, Figure 13 should be regarded only as a means of guiding experiments - for example when determining what region of a fracture map is applicable. This is especially important with regard to engineering alloys, where the presence of precipitate free zones can produce strain localisation and so favour viscous growth.

(iii) A third stage of fracture damage accumulation is observed metallographically when cavities on a particular single grain facet eventually link up to form a distinguishable entity called a 'crack'. As mentioned earlier, this description is to be interpreted liberally since these sgf cracks which are apparent from metallographic observations are such that their number steadily increases as creep strain processes and that their growth is drastically impeded by triple point junctions [8] so much so that the mean value of their thickness to width ratio steadily increases throughout life [8]. Observations have shown that cavitation also occurs throughout the whole lifetime and is therefore concurrent with the appearance of sgf cracks [8]. The plausible conclusion can thus be drawn that cavitation is not uniform on a microscale (as implicitly assumed for example by Greenwood [46] and Raj and Ashby [47]) and that different boundaries, even at the same orientation to the stress axis, cavitate at different rates and consequently give rise to the progressive appearance of sgf cracks. Growth of sgf cracks into mgf cracks may therefore be a matter of chance and Lindborg [48] has produced a statistical model along these lines. However it is an empirical one in the sense that stress components are not included in the model and sgf cracks are created 'instantaneously'. As a consequence the method lacks the generality required for service life prediction purposes but may well prove to be a basis for a more physical theory. One problem of a statistical model is the predicted influence of specimen size whereby an increase in size would give reduced life - whilst, as discussed below, the reverse effect is found.

(iv) The stress components governing the final fracture event have received scant attention by both experimentalists and theoreticians alike. Metallographic investigations have shown that sometimes fracture is due to the propagation of a single crack in a direction perpendicular to the maximum principal stress. Whether this is a direct consequence of an increase in $\sigma_1$, through a reduced section size, or indirectly through a stress concentration at the crack tip is debatable and deserves further

investigation. In other situations failure is apparently by internal necking and the magnitude of $\bar{\sigma}$ clearly should play an important role, but this again has received no more than qualitative experimental support.

Before the stress components can be deduced and the constitutive relations describing final fracture formulated, a more detailed physical appreciation of the fracture event evidently is required than is available at present.

To illustrate the difficulties involved in quantifying final creep fracture Figure 14 shows how the volume fraction of cavitation at fracture varies with fracture elongation. Although all fractures are intergranular, two extreme types can be identified as was mentioned in the introduction. At low ductilities there is every appearance of a 'cracking' type, while at high ductilities the sgf 'cracks' are elongated in the direction of the stress axis and fracture is thought to occur by homogeneous internal rupture. A necessary consequence of this classification is that lifetime should be specimen size dependent for a 'cracking' material but size independent for an internal 'rupturing' material. Figure 14 is also significant in demonstrating that a predictive scheme which relies on a universally constant critical volume fraction of cavities for fracture is clearly invalid.

Webster [49] has made the interesting deduction from creep crack growth studies that, in steels and RR 58, the crack has to be approximately 1 mm in length before any appreciable propagation rate will be achieved under the action of the applied tensile stress through its effect on the stress intensity at the crack tip. Webster concludes that failure in specimens less than approximately 1 mm in thickness must be by another process and he suggests internal collapse due to sgf creep cracks reducing the load bearing capacity. However another possibility is that, in small sections, a crack of sufficient dimensions to cause collapse is formed by statistical linkage of sgf cracks. A corollary is that as the specimen size increases beyond 1 mm statistical linkage may provide insufficient stress amplification to cause collapse and life will become controlled by slow crack propagation and a size effect on lifetime will become apparent. There have been no systematic investigations to establish this, but Taira and Ohtani [18] reported a large increase in lifetime in 18-8 stainless steel as the specimen size was increased. This stainless steel was described as having many 'cracks' and they ascribed the effect to crack growth but offer little proof. Three other materials which showed no evidence of cracking did not show a size effect on life either.

## 5. PREDICTIVE SCHEMES

### a) Design lifetime

Experimental physical metallurgical studies into creep fracture have been conducted mainly under uniaxial tension and have been aimed largely at trying to understand and sometimes quantify creep fracture damage. Cavitation is the type of creep damage most studied and laboratory specimen life predictive theories, based on these studies, have been attempted periodically ever since the seminal paper of Hull and Rimmer [23]. This theory assumed that all cavities were present at the start of the test and that each grew at a rate controlled by the speed of diffusion and linearly proportional to $\sigma_1$. Furthermore, fracture was taken to occur when the cavities occupied the entire area of a grain boundary facet. Subsequent theories have modified two of these assumptions: Greenwood proposed that





cavitation was continuous and related to creep strain [47] and that fracture occurred when the area fraction of cavities was less than unity. More recently, Raj and Ashby [47] introduced time dependent cavity nucleation by applying classical nucleation theory.

The progress in this area is best demonstrated by the predictive scheme of Greenwood [46]. He uses experimental results obtained by himself and Woodford [50,51] which show that the number of cavities per unit area of grain boundary $C_g$ is given by:

$$C_g = j\,\sigma^2\,\epsilon \tag{19}$$

where j is an experimental constant, $\sigma$ is the applied uniaxial tensile stress and $\epsilon$ is the elongation. Growth of each cavity is assumed to be given by:

$$v_c = H\,\sigma\,t \tag{20}$$

where $v_c$ is the volume of an individual cavity, t is time and H is a constant of proportionality. The fracture condition is taken to be that a certain (undefined) proportion of total grain boundary area is occupied by cavities, so that $C_g\,v_c^{2/3} = f$ is the fracture condition, where $f\ (4/3\,\pi^{1/2})^{2/3}$ is the proportion of grain boundary area occupied if all cavities are spherical. Substitution from equations 19 and 20 gives the fracture life $t_f$ as:

$$t_f = \frac{f^{3/2}}{j^{3/2}\,k\,\sigma^4\,\epsilon_f^{3/2}} \tag{21}$$

This theory had the aim of showing that existing knowledge can be assembled into a plausible, quantitative description of the fracture process of a laboratory test specimen rather than of producing an accurate means for predicting service behaviour. Nevertheless, since it reasonably incorporates many factors it can be expected to describe the effect of moderate perturbations within the range of these factors, e.g. within the limits of uniaxial loading. It has been tested against some experimental results obtained with square wave *uniaxial loading* [52] and predicts the behaviour about as well as Kachanov's theory or Robinson's law.

As it stands at the moment, Greenwood's theory cannot account for behaviour under multiaxial loading since the stress component in equation 19 is not defined. Modifications to the theory are therefore necessary before it can possibly account for the observed dependence of fracture lifetime on either $\bar{\sigma}$, $\sigma_1$ or some combination of these two stress components as discussed in section 2. A recent study of creep of Nimonic 80A in tension and torsion at 750°C [53] showed that both $\sigma_1$ and $\bar{\sigma}$ were required to describe fracture in this material over a wide stress range. As regards cavitation damage, the main effect of stress system was to influence the number of cavities produced per unit of strain at given $\bar{\sigma}$. In explanation of this it appears reasonable, as mentioned earlier, to suppose that during each element of strain, cavities of a range of sizes are nucleated, of which only those with radius $r = 2\,\gamma/\sigma_1$ are stable in the sense that thermodynamics enables them to grow instead of to shrink. The larger $\sigma_1$ the greater is the proportion of these cavities that are permanent. Experiment showed that at constant $\bar{\sigma}$, $C_v \propto \sigma_1^2$, where $C_v$ is the number of cavities per unit volume and thus expresses the observation that approximately

3 times as many cavities are found in tension as in torsion after creeping to the same strain at the same $\bar{\sigma}$.

An important feature of the creep data was that steady state creep occupied only about 10% of lifetime although the magnitude of the minimum creep rate was dependent only upon $\bar{\sigma}$, as deformation theory predicts. Tertiary creep on the other hand set in earlier in tension than in torsion and was therefore a function of $\bar{\sigma}$ and $\sigma_1$ and consequently led to a shorter life in tension than in torsion. To explain this creep and fracture behaviour, it was hypothesised that cavities accelerated the creep rate and thus, in effect, softened the metal. Since there were too few cavities, even at fracture, to cause a significant reduction of cross sectional area (that is, no effect on w) the softening was ascribed to an accelerating effect on recovery and thereby implying a cavity growth law $\dot{v}_c \alpha \dot{\epsilon}$ rather than $\dot{v} \alpha \sigma_1$. Two constitutive relations were deduced:

$$\dot{\bar{\epsilon}} = P\, v^{4/3} \tag{22}$$

$$\dot{v} = Q\, (\bar{\epsilon})^{7/6} \tag{23}$$

where $\epsilon$ is the effective tertiary creep rate, v is the total cavity volume, P is a function of $\bar{\sigma}$ and Q a function of $\bar{\sigma}$ and $\sigma_1$. Combining equations 22 and 23 gives the tertiary creep law $\dot{\bar{\epsilon}} = R\, t^3$ which is close to experiment and R contains the correct fucntions of $\bar{\sigma}$ and $\sigma_1$. More importantly for the present, equations 22 and 23 can be used to predict fracture life $t_f$ as

$$t_f = \frac{A}{(\bar{\sigma})^{q-1.8}\sigma_1^{\,2}} \tag{24}$$

Here A is a function of $\bar{\sigma}$ and q is the exponent in a Norton law type of equation for cavity volume fraction. The dotted lines in Figure 15 are calculated from equation 24 for tension and torsion and the points are from tension and torsion experiments. The agreement is satisfactory. Further, in the middle range of stress, q = 4 and equation 24 then gives the line labelled B in Figure 10.

It is worth emphasising that, according to the experimental observations just mentioned, cavitation and also sgf crack damage weakens the metal by 'softening' rather than by reducing the effective cross-sectional area, as Kachanov's theory supposes.

Since, in Nimonic 80A, the degree of cavitation increases as the stress state changes from torsion to tension then a further increase in cavitation rate is predicted on going to a triaxial tensile stress state. As discussed in section 2, a spatially significant and well defined triaxial tensile stress state can be achieved in a circumferentially notched bar by judicious matching of notch geometry and creep behaviour. Dyson and Rodgers [54] have employed this technique and Figure 16 shows that there are indeed more cracked boundaries (the number of discrete cavities could equally well have been plotted) in the centre of the specimen where $\sigma_1/\bar{\sigma}$ (given as $\sigma_a/\bar{\sigma}$ in Figure 16) is largest.

(b) Residual life

Some components in existing plant suffer temperature and stress excursions within limits that may be known quite accurately although the precise times





at these temperatures and stresses may not.

In order to maximise the useful life it is necessary to make periodic estimates of residual life. When fracture or useful life is controlled by an internal damage process then it becomes possible as a result of identifying damage to estimate the residual lifetime from metallographic observations. This possibility has been used so far only in connection with cavitation damage. A number of industrial organizations make practical qualitative assessments by observing the degree of cavitation or sgf crack damage but quantitative estimates now seem quite possible in those cases where cavitation damage exists for a large fraction of the life [55]. For example, given information such as that in Figure 17, residual life can be estimated by counting the number of cavities on a metallographic section. Considerable innovatory work is still needed in view of the difficulties encountered with another material [37] but, as compared with the method of estimating residual life from the deterioration in breaking strength, which is sometimes used, the metallographic method requires a smaller sample to be detached from the component and probes directly the significant damage. It therefore promises to be inherently more reliable but, the process of selection of the metallographic specimen can cause major practical problems because the critically damaged region may be hard to locate.

Significant work on the extension of residual life via heat treatment of small components, temporarily taken from service, has been carried out and Wilshire and Dennison report further work at this conference [56].

## 6. FUTURE WORK AND CONCLUSIONS

There are several types of investigation which would extend the help already available from metal science for improving the prediction of creep life and a few of these are singled out below.

1. A conclusion from section 4 is that the ratio

$$\frac{\sigma_1}{\bar{\sigma}}$$

or equivalently $\sigma_1/\tau_{oct}$ characterises the type of stress system as far as creep under *service* stresses is concerned. Some conclusions about multiaxial testing follow as a consequence. In Figure 18 the curves show $\tau_{oct}/\sigma_1$ as a function of $\sigma_2/\sigma_1$ with the third stress $\sigma_3 = \nu(\sigma_1 + \sigma_3)$. The upper curve is for $\sigma_3 = 0$; along this curve $\tau_{oct}/\sigma_1$ changes considerably in the range $-1 < \sigma_2/\sigma_1 < 0$, i.e. between torsion and uniaxial tension, but changes little in the range $0 < \sigma_2/\sigma_1 < 1$, i.e. between uniaxial and biaxial tension, which covers the stress systems obtained with pressurised thin tubes or cruciform biaxial specimens. It seems doubtful if the small changes in $\tau_{oct}/\sigma_1$ achievable are worth the extra complexity in the testing. With triaxial tension the conclusion is different, as is also evident in Figure 18 especially from the bottom line for which $\sigma_3 = 1/2\ (\sigma_1 + \sigma_2)$; along this line, over the range $0 < \sigma_1/\sigma_2 < 1$, $\tau_{oct}/\sigma_1$ falls to zero. Since stress systems in this range probably include the most dangerous systems encountered in service, quantitative studies of cavitation in triaxial tension are particularly needed

2. The growth of cavities needs fuller examination. As mentioned, it has generally been assumed that their growth rate is diffusion controlled, which results in a volume growth rate $\dot{v}_c \alpha \sigma_1$, but recent experimental work with two different engineering materials [53,57] indicates $\dot{v}_c \alpha (\bar{\sigma})^n$.

Predictions concerning design lifetime, either under variable or multiaxial stress and especially the important prediction from short-time tests to service-life-times, involve this growth law, which is therefore important. What is needed are experimentally checked *Cavity Growth Maps* covering the regimes for the different types of diffusional and viscous (power law creep) growth.

3. The initiation and growth of *cracks* which can be treated by the various theoretical techniques available to the fracture mechanician needs further study. As discussed, in some materials a crack forms, perhaps by chance linkage of neighbouring small cracks, of sufficient length that it can grow under the direct action of the maximum principal stress. This marks the initiation properly-called of a crack, and divides the creep life into an earlier part during which the main damage was cavitation and single and multiple grain facet cracking, and a later part in which the significant damage consists of one dominant crack. The mechanics and mechanisms of initiation of such cracks needs further study; their propagation behaviour having received considerable attention recently [3,4]. In large components, which form a small but expensive part of all those subject to creep, it is conceivable that most of the lifetime may be occupied by the growth stage of such a crack but, at present, no scientific judgement can be exercised in this respect at the design stage of the component.

4. Metal science studies [55] have already demonstrated the potential that exists for quantitative estimates of residual lifetime by measuring cavitation damage. There is a need for more extensive studies to identify and quantify the relevant damage parameter in other important engineering alloys so that the scope and limitations of this method can be assessed. As an example, in Inconel X-750 it has been shown [8] that single and multiple grain facet cracks exist for about 90% of life in fine grained material and their measurement therefore may form the basis of a residual life technique. In coarse grained material, sgf cracks only occupy a small fraction of life and cavitation may well provide a better assessment. Figure 19 illustrates the point in schematic form.

5. The main gain would come, undoubtedly, from an integrated metal science and mechanics (including fracture mechanics) approach, to the problems raised by predictive requirements, e.g. the behaviour of alloys under triaxial tensile stress, under variable conditions, with simultaneous environmental attack etc. It is hoped that this present paper has established that this integration is both feasible and appropriate.

ACKNOWLEDGEMENTS

This work forms part of a collaborative project between the National Physical Laboratory and the University of Waterloo. The work at Waterloo is supported by the National Research Council of Canada. Discussions with co-workers are acknowledged with pleasure.





REFERENCES

1. COFFIN, L. F., Jr., Fracture 1977, (ed. D. M. R. Taplin), Volume I, University of Waterloo Press, Canada.
2. GREENWOOD, G. W., Fracture 1977, (ed. D. M. R. Taplin), Volume I, University of Waterloo Press, Canada.
3. KUHN, H. and DIETER, G. E., Fracture 1977, (ed. D. M. R. Taplin) Volume I, University of Waterloo Press, Canada.
4. NIKBIN, K. M., WEBSTER, G. A. and TURNER, C. E., Fracture 1977 (ed. D. M. R. Taplin) Volume II; JONES, C. L. and PILKINGTON, R., Fracture 1977, Volume II, University of Waterloo Press, Canada.
5. KNOTT, J. F., Fracture 1977, (ed. D. M. R. Taplin), Volume I, University of Waterloo Press, Canada.
6. ASHBY, M. F., Fracture 1977, (ed. D. M. R. Taplin), Volume I, University of Waterloo Press, Canada.
7. McMAHON, C. J., Jr., Fracture 1977, (ed. D. M. R. Taplin), Volume I, University of Waterloo Press, Canada.
8. VENKITESWARAN, P. K. and TAPLIN, D. M. R., Met. Sci. 8, 1974, 97.
9. FLECK, R. G., BEEVERS, C. J. and TAPLIN, D. M. R., Met. Sci. 9, 1975, 49.
10. GOODS, S. H. and NIX, W. D., Fracture 1977, (ed. D. M. R. Taplin), Volume II, University of Waterloo Press, Canada.
11. McLEAN, D., Rep. Progress in Physics, 1, 1966.
12. RICE, J. R., Gordon Conference on Fracture 1975, Brown University, Rhode Island, U.S.A.
13. JOHNSON, A. E. and HENDERSON, J., Complex-stress creep, relaxation and fracture of metallic alloys, HMSO Edinburgh, 1962.
14. JOHNSON, A. E., Recent progress in Applied Mechanics (ed. B. Broberg) John Wiley, 1967, 289.
15. FINNIE, I. and ABO EL ATA, M., Advances in Creep Design (ed. Smith and Nicolson) Applied Science, 1971, 329.
16. SIEGFRIED, W., J. Appl. Mech. 10 (4), 1943, 202.
17. KOCHENDORFER, A. and ROHRBACH, C., Arch Eisenhüttenw 26, 1955, 213.
18. TAIRA, S. and OHTANI, R., Advances in Creep Design, (ed. Smith and Nicholson) Applied Science, 1971, 289.
19. HENDERSON, J. and SNEDDON, J. D., DTI Natn. Engng. Lab. Rep. No. 509, 1972.
20. HAYHURST, D. R., J. Mech. Phys. Solids 20, 1972, 381.
21. LECKIE, F. A. and HAYHURST, D. R., Proc. Roy Soc. Lond. A340, 1974, 323.
22. KELLY, D., Acta Met 23, No. 10, 1975, 1267.
23. NEEDHAM, N. G. and GREENWOOD, G. W., Metal Science 9, 1975, 258.
24. JOHNSON, A. E., HENDERSON, J. and MATHUR, V. D., Engineer. Lond. 202 (5248) 261; 202 (5249) 299.
25. HULL, D. and RIMMER, D. E., Phil. Mag. 4, 1959, 673.
26. DAVIS, E. A. and MANJOINE, J. J., Amer. Soc. Test. Mater. STP No. 128, 67.
27. TAIRA, S. and OHTANI, R., Int. Conf. on Creep and Fatigue, 1973, Paper C213/73.
28. (a) HAYHURST, D. R. and LECKIE, F. A., Univ. of Leicester Eng. Dept., Report 75-2, April, 1975; (b) HAYHURST, D. R. and HENDERSON, J. T., Univ. of Leicester Eng. Dept., Report 76-2, May, 1976; (c) HAYHURST, D. R., LECKIE, F. A. and HENDERSON, J. T., Univ. of Leicester Eng. Dept., Report 76-3, May, 1976.
29. BRIDGMAN, P. W., Large Plastic Flow and Fracture, McGraw Hill, 1952.
30. KACHANOV, M., Izv Adad Nauk, SSSR OTN, No. 8, 1958, 26.
31. PENNY, R. K., Metals and Materials 8, 1974, 278.

32. RABOTNOV, Yu, N., Advances in Creep Design, (ed. Smith and Nicolson), Applied Science, 1971, 11.
33. DYSON, B. F. and TAPLIN, D. M. R., Inst. of Metallurgists Conf. on Grain Boundaries, Jersey, April 1976, Paper E23.
34. WEBSTER, G. A. and PIERCEY, B. J., Trans. Am. Soc. Met. Quarterly, 59, 1966, 847.
35. HALE, K. F., Conf. on Phys. Met. of Reactor Fuel Elements, Met. Soc. London, 1973, 193.
36. PERRY, A. J., J. Materials Science, 9, 1974, 1016.
37. TIPLER, H. R. and HOPKINS, B. E., Met. Sci., 10, 1976, 47.
38. BISHOP, J. F. W. and HILL, R., Phil. Mag., 42, 1951, 1298.
39. DYSON, B. F., LOVEDAY, M. S. and RODGERS, J. M., Proc. Roy. Soc. London A349, 1976, 245.
40. HARRIS, J. E., Trans. AIME, 233, 1965, 1509.
41. SPEIGHT, M. V. and HARRIS, J., Met. Sci. J., 1, 1967, 83.
42. DAVIES, P. W. and WILSHIRE, B., Structural Processes in Creep, London ISI, 1961, 34.
43. ISHIDA, Y. and McLEAN, D., Met. Sci. J., 1, 1967, 171.
44. DYSON, B. F., Metal Science, 10, No. 10, 1976, 346.
45. HANCOCK, J. Metal Science, 10, No. 10, 1976, 319.
46. GREENWOOD, G. W., Int. Conf. on Metals, Cambridge, 1973, 91.
47. RAJ, R. and ASHBY, M. F., Acta Met., 23, 1975, 653.
48. LINDBORG, U., J. Mechanics and Physics Solids, 16, 1968, 323.
49. WEBSTER, G. A., The Mechanics and Physics of Fracture, Inst. of Physics and Metals Society, Paper No. 18, 1975.
50. WOODFORD, D. A., Met. Sci. J., 3, 1969, 50.
51. WOODFORD, D. A., Met. Sci. J., 3, 1969, 234.
52. DYSON, B. F., GIBBONS, T. B. and McLEAN, D., NPL Report IMS 30, 1975.
53. DYSON, B. F. and McLean, D., Metal Sci., 1977, to appear.
54. DYSON, B. F. and RODGERS, M. J., to be published.
55. DYSON, B. F. and McLEAN, D., Metal Sci. J., 6, 1972, 220.
56. DENNISON, J. P. and WILSHIRE, B., Fracture 1977, (ed. D. M. R. Taplin) Volume II, University of Waterloo Press, Canada.
57. CANE, B. J., Conf. on Grain Boundaries, Jersey, 1976, paper E7.





Table 1

| Type of Copper | Grain Size μ | Temperature range °C | Fracture time relation $t_f$ (h) | Reference |
|---|---|---|---|---|
| Commercially pure | 90 | 250 | $t_f = 1.6 \times 10^5 \exp(-0.1\sigma_1)$ $10^4 \geq t_f \geq 200h$ | Johnson et al [24] |
| Electrolytic tough pitch | 40 | 250 | $t_f = 3.8 \times 10^6 \exp(-0.021\sigma - 0.06\sigma_1)$ $130 \geq t_f \geq 30h$ | Finnie and Abo El Ata [15] |
| BS 2874 0.1% $O_2$ tough pitch | 150 | 250 | $t_f = 8.7 \times 10^3 \exp(-0.09\sigma_1)$ $2 \times 10^3 \geq t_f \geq 10h$ | Kelly [22] |
| 99.8% pure | not given | 400-500 | $t_f^{400°C} = A \exp(-0.2\bar{\sigma} - 0.07\sigma_1)$ $10 \geq t_f \geq \frac{1}{2}h$ | Hull and Rimmer [25] |
| OFHC | 230 | 500 | $t_f = 1.8 \times 10^{\frac{1}{2}} \exp(-0.18\sigma_1)$ $3 \times 10^3 \geq t_f \geq 40h$ | Needham and Greenwood [23] |

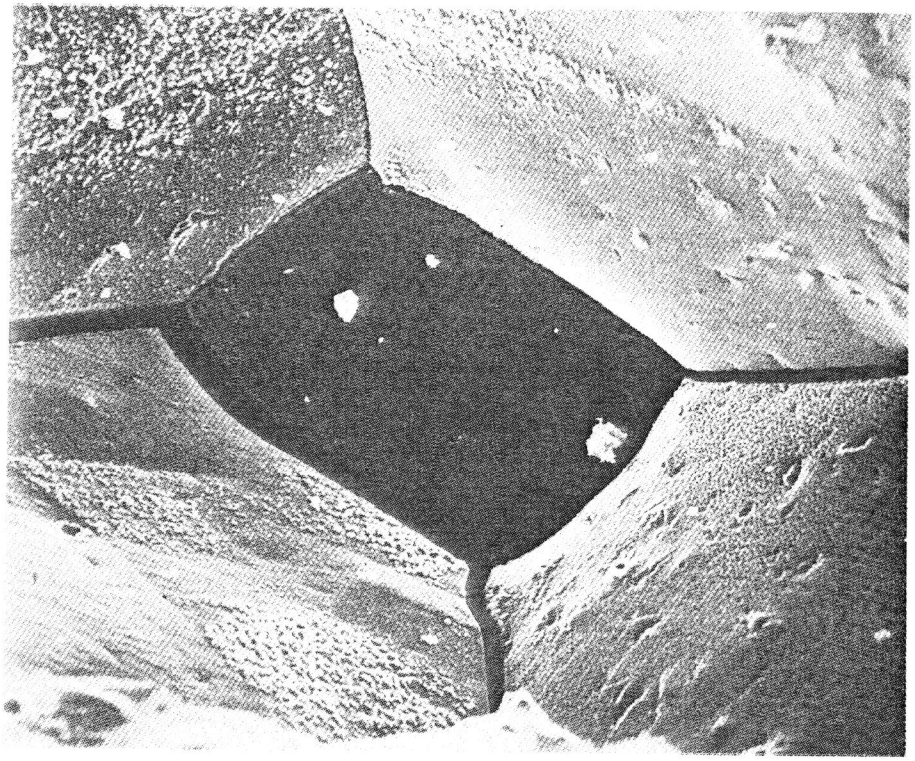

Figure 1 Scanning electron micrograph showing typical appearance of the fracture surface in a 'brittle' alloy. Inconel X-750 creep tested at 973 K, grain size 113 μm; secondary creep rate 0.76 m/m/s. X 2000



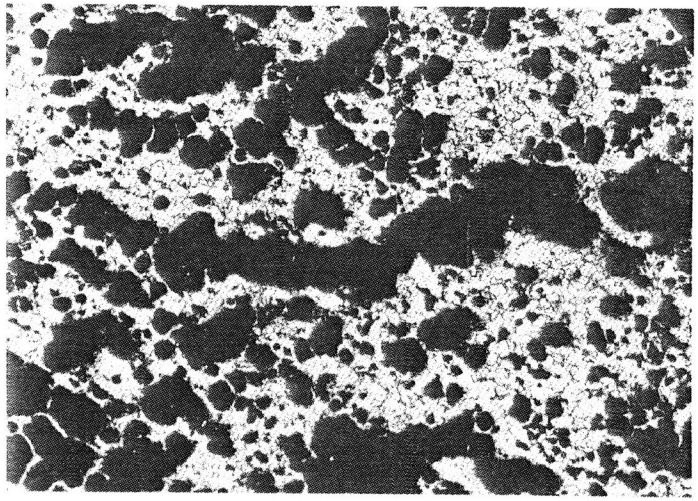

Figure 2 Optical micrograph showing the fracture process in a 'ductile' alloy. Alpha/Beta brass tested at 873 K. Courtesy of Acta Metallurgica. X 75

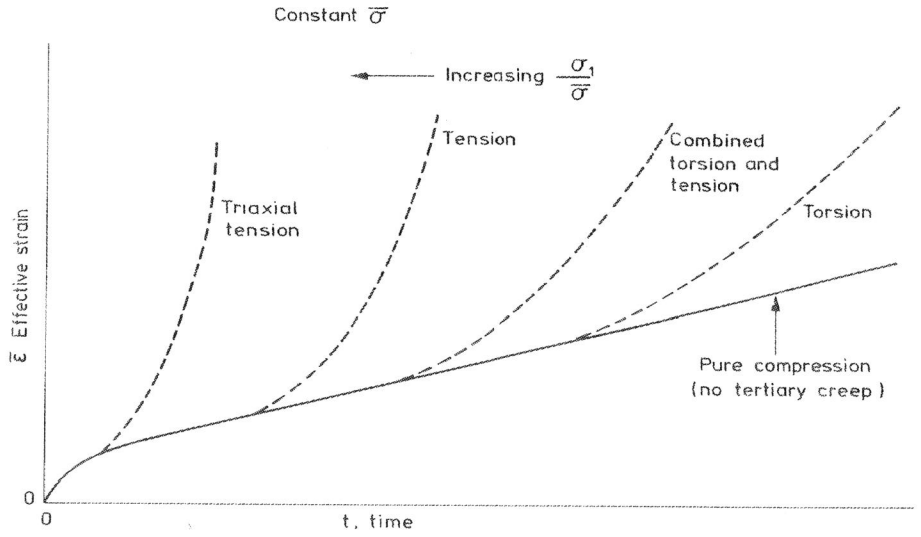


Figure 3 Schematic representation of the shapes of creep curves for constant shear stress $\bar{\sigma}$ but with different values of the stress state parameter $\frac{\sigma_1}{\bar{\sigma}}$ predicted by equation 6.

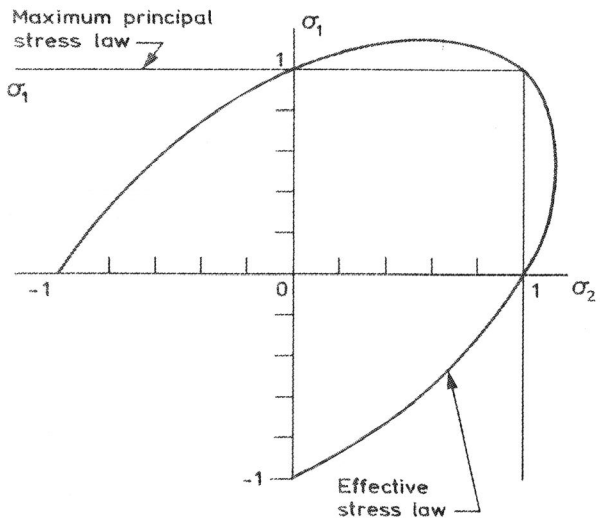


Figure 4 Two plane stress isochronous rupture surfaces for materials which obey either (a) the maximum principal stress law or (b) the effective stress law.

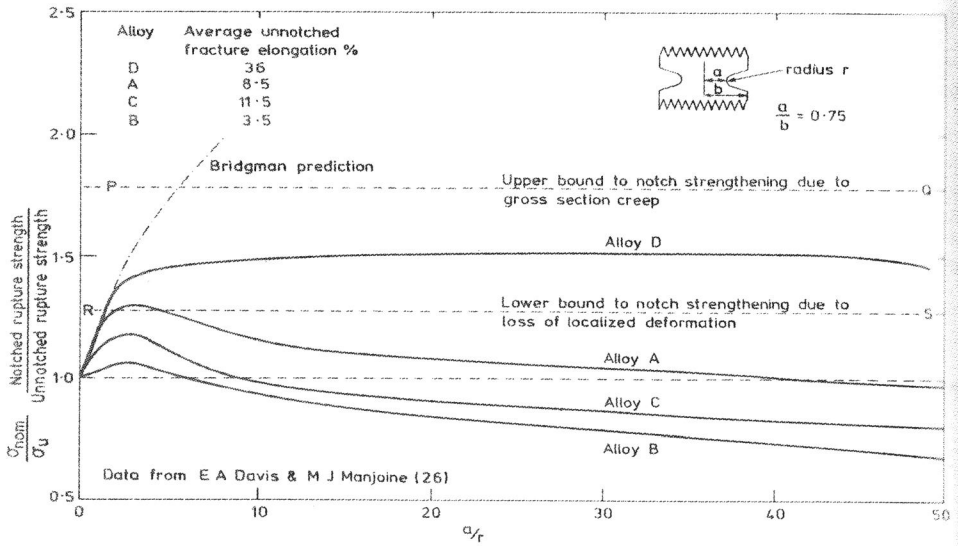


Figure 5 A plot of the ratio of notched to unnotched rupture strength against notch sharpness for four different alloys. Data from Davis and Manjoine [26].





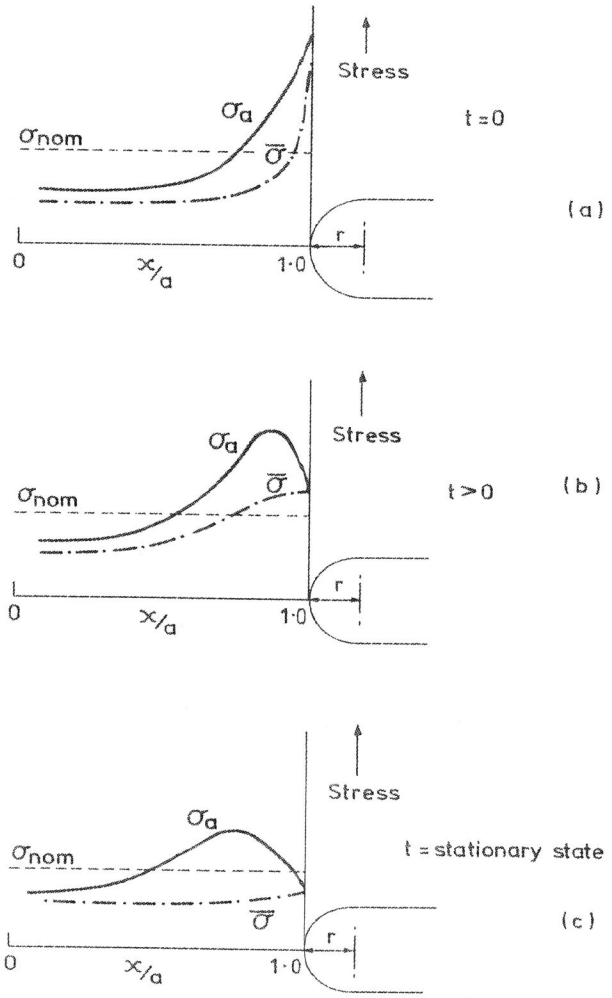


Figure 6 Schematic representation of: (a) initial elastic (b) transient and (c) stationary state stress distributions in the throat section of a circumferentially notched bar.

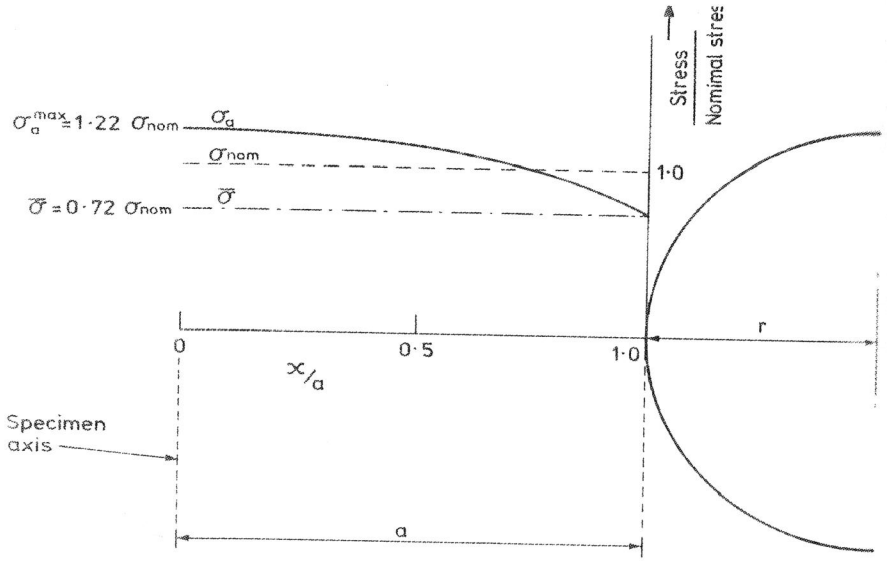


Figure 7 Axial and effective stress distribution in the throat section of a circumferentially notched bar with a 'Bridgman' notch geometry. $a/_{2r} = 1$.

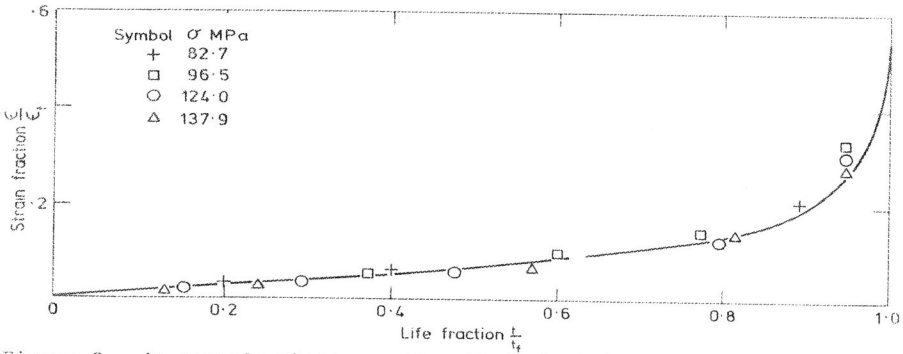


Figure 8 An example where equation 10 derived from Kachanov's theory agrees with experiment. The experimental data (points) are for an Aluminium alloy and the solid line is from equation 10 with n = p = 5 (after Penny [31]).





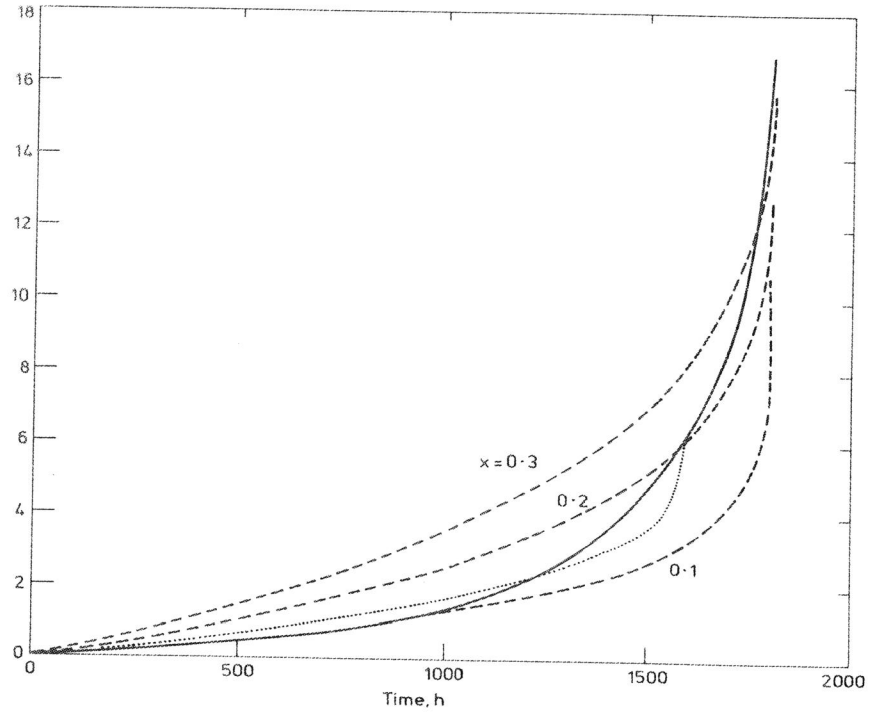


Figure 9 An example where equation 10 does not agree with experiment. The solid line is the experimental curve for Nimonic 80A in tensile creep at 750°C and $\sigma_1$ = 154 MPa and the dashed lines are calculated from equation 10 with n = p; x = 1/(1+n)

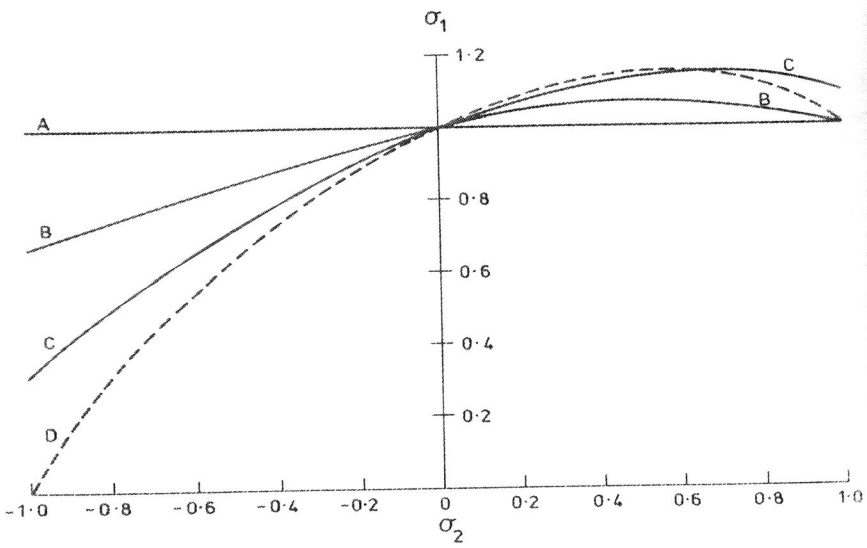


Figure 10 Shapes of isochronous fracture surfaces in plane stress. A and C from Kachanov with the two different assumptions about damage rate. D. when $t_f$ depends only on $\bar{\sigma}$. B, for Nimonic 80A from metallographic studies.





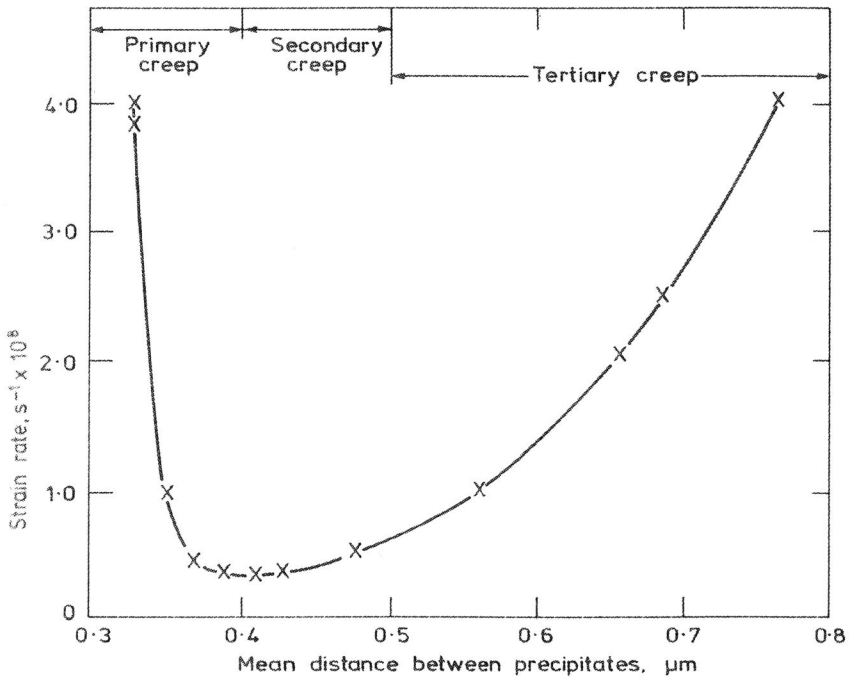


Figure 11 Creep rate plotted against distance between precipitate particles. 2 1/4%Cr-1%Mo superheater tube alloy in tensile test at 650°C and 35 MPa (Hale [35]).

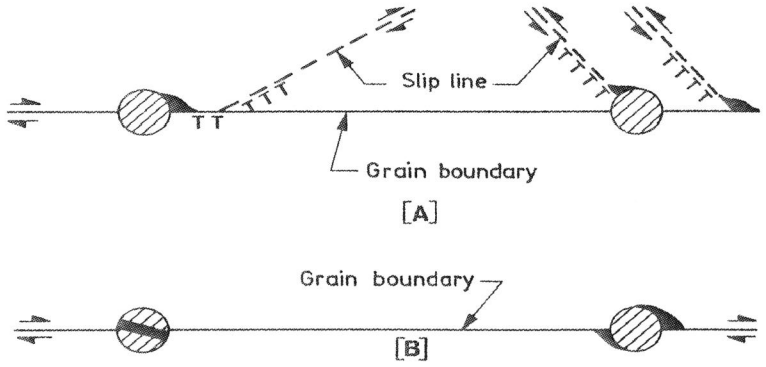


Figure 12 Schematic diagram illustrating nucleation mechanisms which have some experimental support.

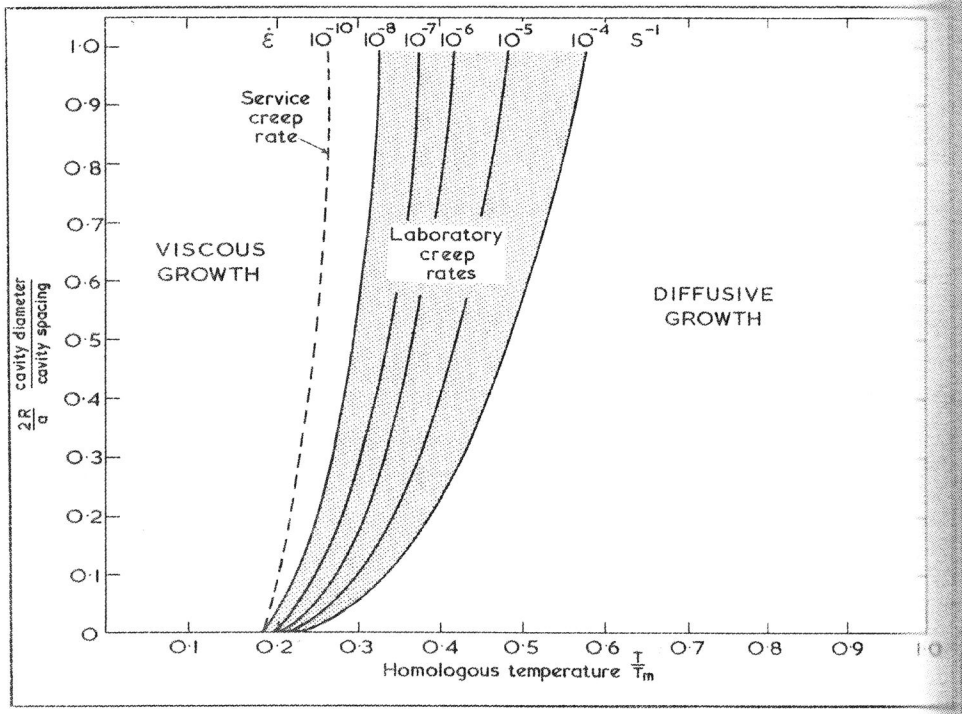


Figure 13 Non-Newtonian viscous and diffusive cavity growth regimes as a function of temperature and the ratio of cavity diameter to to cavity spacing for different creep rates.





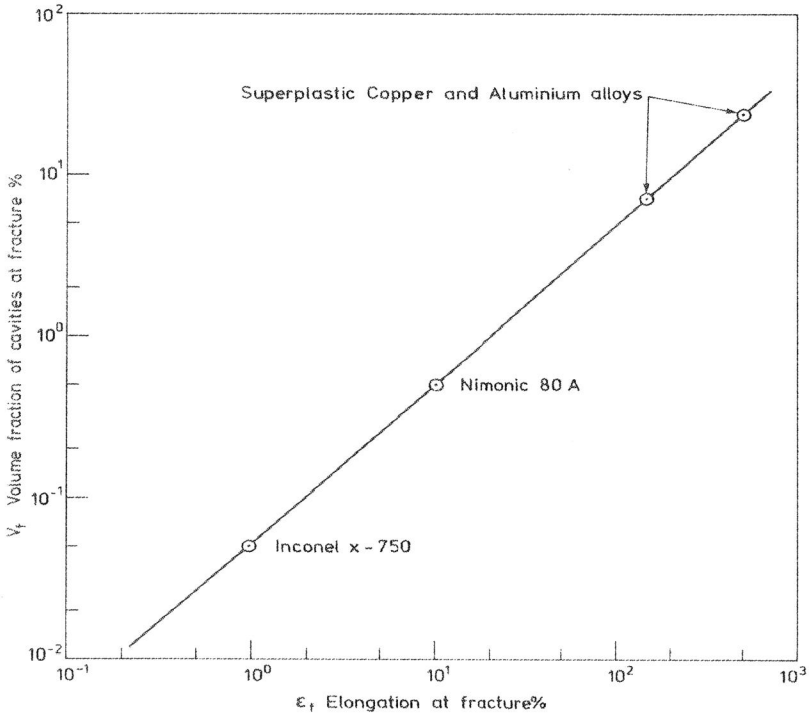


Figure 14 Volume fraction of cavities at fracture of four materials exhibiting widely differing elongations at fracture.

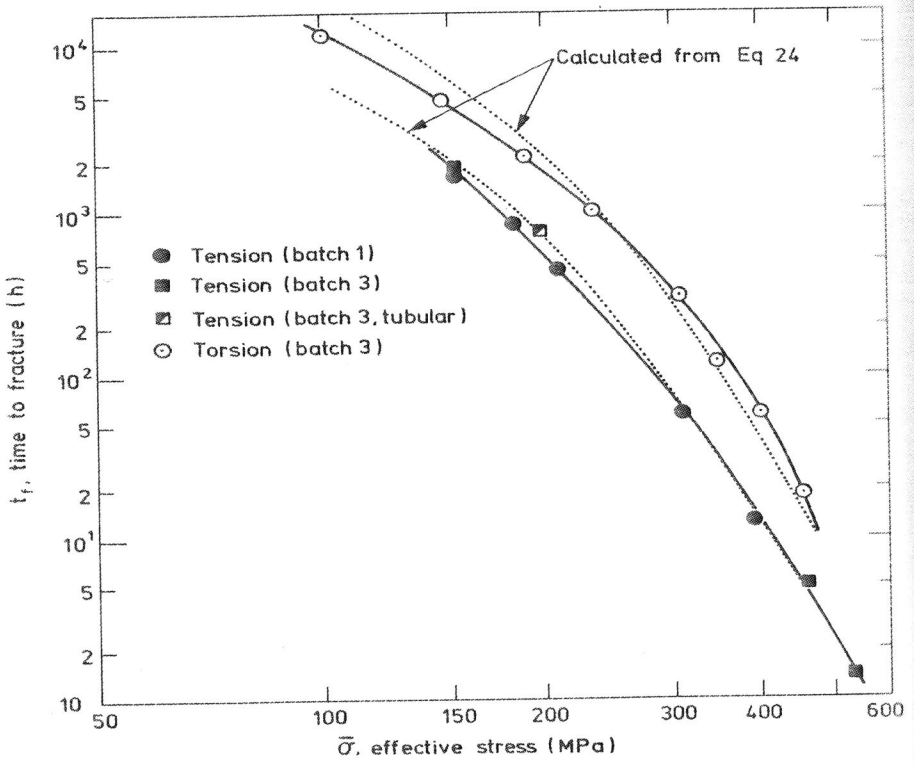


Figure 15 Dotted lines - $t_f$ calculated from equation 24, which is based on metallographic observations. Points on solid lines - experimental data. Tension and torsion tests on Nimonic 80A at 750°C.





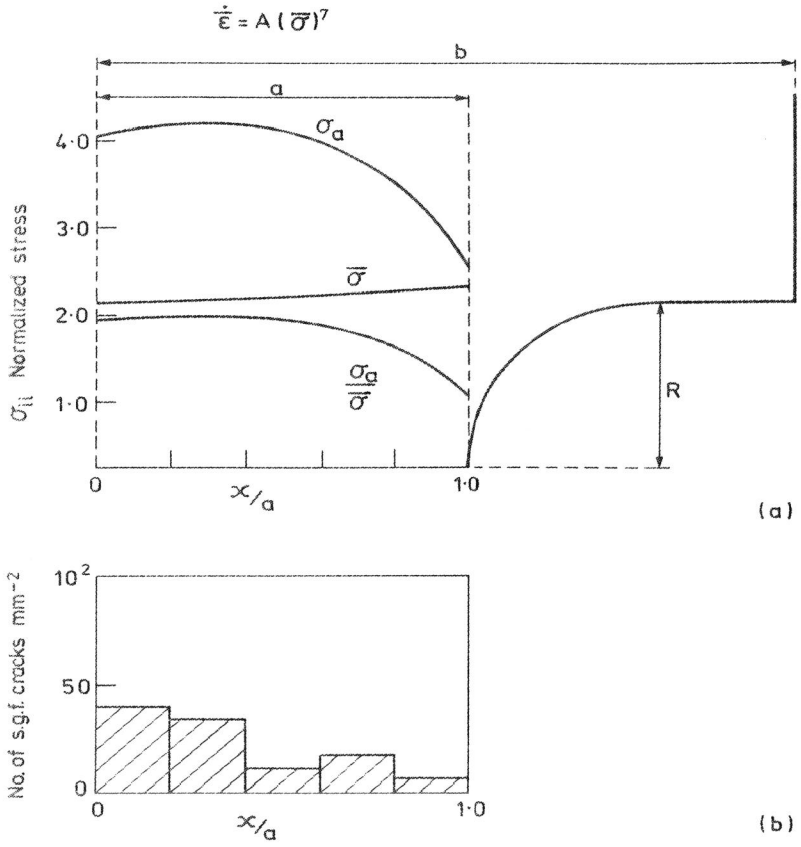


Figure 16 (a) shows the spatial variation of the stationary state axial and effective stresses across the throat of a notch characterised by $^b/_a$ = 1.9 and $^R/_a$ = 0.5 (Data from Hayhurst and Leckie [28a]. (b) shows effect of increasing triaxial tension (represented by large values of $^{\sigma}a/\bar{\sigma}$) on the rate of creation of cavitation damage. The specimen was interrupted at $^3/4$ lifetime. (Data from Dyson and Rodgers [54]).

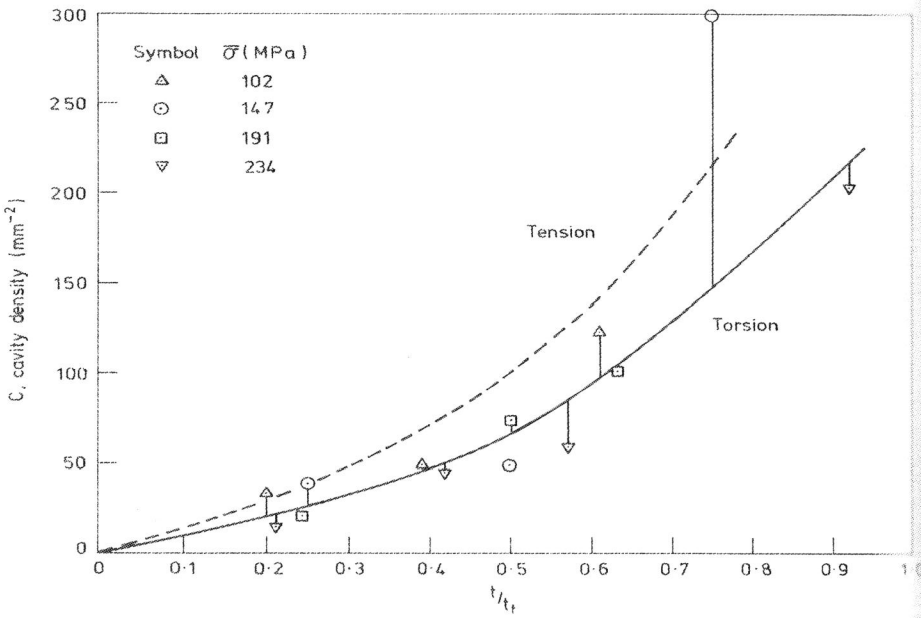


Figure 17 Number of cavities c plotted against fractional life $t/t_f$. Dashed line represents mean of tension data [53]. Such data promise a quantitative estimate of residual life possessed by a component still in service.





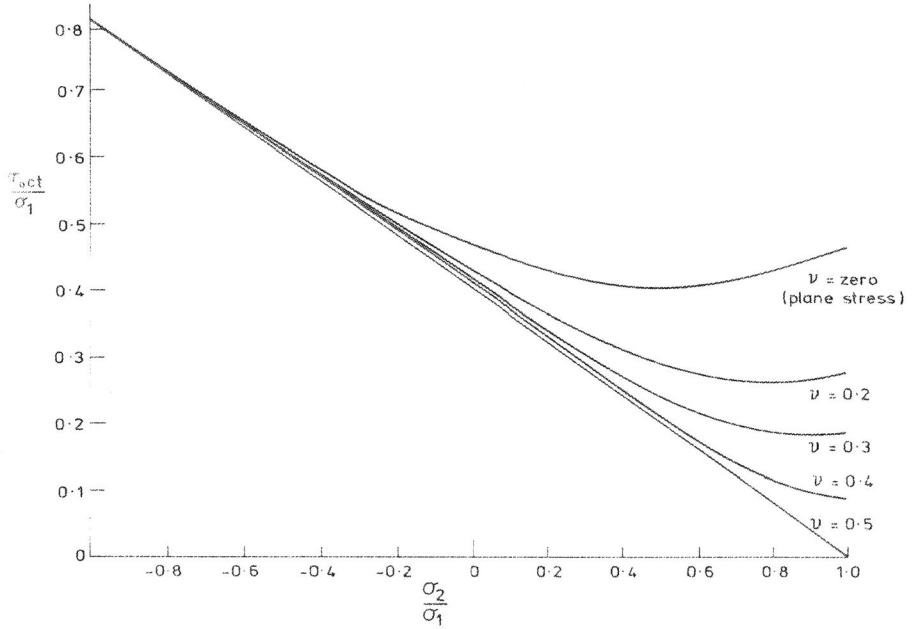


Figure 18 $\tau_{oct}/\sigma_1$ vs $\sigma_2/\sigma_1$ for different values of $\sigma_3 = \nu(\sigma_1 + \sigma_2)$.

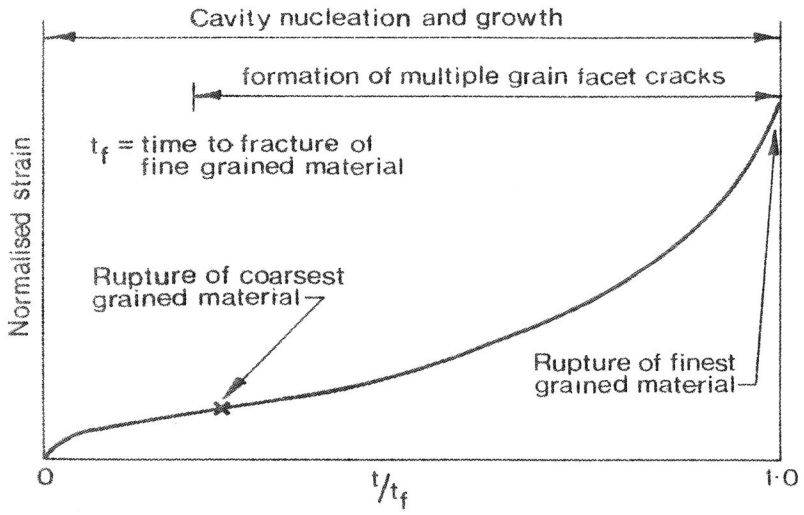


Figure 19 Schematic diagram illustrating the fact that single and multiple grain facet cracks in Inconel X-750 occupy an increasing fraction of the lifetime as grain size is reduced. Based on work of Venkiteswaran and Taplin [8].